

## Welding of Wood in the Presence of Wollastonite

Mojgan Vaziri,<sup>\*,a</sup> Lars Abrahamsson,<sup>b</sup> Olle Hagman,<sup>a</sup> and Dick Sandberg<sup>a</sup>

The use of wollastonite as a natural additive for the welding of Scots pine improved the water resistance and shear strength of the welded joint. The X-ray computed tomography images revealed that the welding of Scots pine with wollastonite could postpone crack formation in the welded joints. The specimens welded for a longer time (5 s) had a more uniform distribution of wollastonite particles in welded joints. The microstructure of the wood and the thickness of the wood cell walls also had a great influence on the thickness and strength of the welded joints. Water immersion tests showed that the use of wollastonite in wood joints was able to meet the requirement of resistance to frequent short-term and long-term exposure to water.

*Keywords:* Cracking; CT scanning; Micro CT scanning; Shear strength; Water immersion; Welding time

*Contact information:* a: Luleå University of Technology (LTU), Wood Science and Engineering, Forskargatan 1, 931 87, Skellefteå, Sweden; b: Vattenfall AB, BU Fuel, Engineering & Projects, Evenemangsgatan 13, 169 79 Solna, Sweden; \*Corresponding author: Mojgan.vaziri@ltu.se

### INTRODUCTION

Wood welding is an innovative technology that makes it possible to join wood pieces by frictional movement between the two surfaces under an external pressure, which results in an increase in the interfacial temperature and the softening of wood components. Solidification of the flow-induced material at the interphase results in a bond capable of reproducing the behavior and performance of a synthetic resin. Friction welding is an environmentally compatible assembling and manufacturing process that only requires short processing time, and does not use synthetic adhesives or any special processes to prepare the wood surfaces. However, there are few studies so far related to structural applications, which is partially due to the vulnerability of the weld to damage from moisture.

Some methods for enhancing the moisture resistance of welded wood joints have been studied by Pizzi *et al.* (2011), Amirou *et al.* (2017), and Mansouri *et al.* (2011), who searched to find additive compounds capable of waterproofing the welded joints. Nearly all the earlier studies indicated that there is a lack of basic understanding of the underlying mechanisms of water permeation in the welded joints, which leads to poor results from attempts to modify the water permeability of these products.

One hypothesis that could explain the poor water resistance of the welded joints is that uneven swelling of the welded area and of the adherent non-welded wood causes severe stresses that crack and open the welded joints (Vaziri *et al.* 2019a). Weak chemical and mechanical bonds between the welded joint and the adherent wood, as well as heterogeneous heat distribution in the welded interphase during the welding process, could be other reasons contributing to the poor durability of the welded wood joints (Vaziri *et al.* 2014).

The present investigation was designed to study the effect of pretreating the welding interphase with wollastonite as a natural alternative compound and using two

different welding times. A crack in the welded joint is assumed to be the first sign of damage. Through non-destructive test methods, such as X-ray computed tomography (CT-scanning) and micro CT-scanning, the formation of cracks in the welded joints and the micromorphology of the welded interphases were studied. In addition, the shear strength of the welded wood and the durability of the weld in water have been investigated.

Wollastonite is the name for a type of calcium silicate ( $\text{CaSiO}_3$ ) mineral that exists in a fibrous needle-shaped (acicular) form and is formed by contact metamorphism of limestone. The chemical composition of wollastonite is mainly 48.3% calcium oxide (CaO) and 51.7% silicon dioxide ( $\text{SiO}_2$ ). Traces of aluminum oxide ( $\text{Al}_2\text{O}_3$ ), magnesium (Mg), and potassium (K) may be found in this mineral compound (Maxim and McConnell 2005). Although the absolute thermal conductivity of wollastonite is low, its value is relatively high in combination with other materials, such as wood or plastics; the addition of wollastonite can increase the thermal conductivity of the resulting composite (Karimi *et al.* 2013).

One mechanism by which wollastonite could contribute to an improved welded joint is that the wollastonite particles can increase the friction and heat generation at the weld's interphase. This, in turn, can increase the degradation of wood constituents, which can increase flow-induced material at the interphase that leads to better adhesion at the joint. The wollastonite particles may also participate as reinforcement in a nanocomposite structure at the welded interphase region.

## EXPERIMENTAL

### Materials

#### *Preparation of specimens for welding*

Wood specimens with the dimensions of 20 mm × 20 mm × 230 mm (radial (R) × tangential (T) × longitudinal (L)) were prepared from clear pieces of Scots pine (*Pinus sylvestris* L.) grown in northern Skellefteå, Sweden. The specimens were conditioned for two weeks at 20 °C and 65% relative humidity (RH) in an environmental chamber to 12% moisture content (MC) and welded together in pairs to dimensions of 20 mm × 40 mm × 230 mm (*i.e.*, longitudinal welding of a tangential face to a radial face). One surface (20 mm × 230 mm) of each pair was evenly covered by 0.2 g of wollastonite powder just before welding them together. The linear vibration-welding machine, Branson model M-624 (Branson Ultraschall, Dietzenbach, Germany), was set to a frequency of 240 Hz and to the most important parameter settings listed in Table 1.

**Table 1.** Welding Procedure and Classification of the Specimens

Welded Specimens		Welding Times S1 + S2 (s)	Holding Time (s)	Initial Welding Pressure (MPa)	Second Welding Pressure (MPa)	Holding Pressure (MPa)
With Wollastonite	Without Wollastonite (Controls)					
W4	R4	2 + 2	10	1.3	1.7	2.7
W5	R5	2 + 3				

The wollastonite used in this study was a minimally refined powder that consisted of a mixture of various sizes of acicular particles (with a large proportion of the particles being approximately 0.05 to 0.1 mm in the longest direction). The wollastonite powder was

sourced from the Svårtsångs mine in Filipstad, Sweden, Sweden. Two types of specimens were prepared; those welded with wollastonite using two different welding times (W4, W5) and those welded without wollastonite (R4, R5), which served as the controls.

## Methods

### CT scanning

The welded specimens were conditioned for two weeks at 20 °C and 65% RH in an environmental chamber to 12% MC before they were scanned. For each welding time and corresponding control specimen there were five replicates, so in total 20 specimens were prepared and then placed with their butt ends in 5-mm-deep tap water in an experimental rig (Fig. 1). The specimens were scanned over four days at 30 min intervals using a medical X-ray CT scanner (Siemens Emotion Duo; Siemens Healthcare GmbH, Erlangen, Germany) at ambient conditions with the scanner settings listed in Table 2. The standard algorithm of the Shepp-Logan kernel was used for the image reconstructions (Shepp and Logan 1974). The X-ray absorptions of the pixels were averaged along the direction perpendicular to the welded areas. Each averaged area had the dimensions of 222 mm × 12.9 mm to have margins for tilting and swelling specimens.

**Table 2.** Setting of the CT Scanner

Parameter	Unit	Value
Voltage	kV	110
Current	mA	70
Scan time	s	2
Scan thickness	mm	1
Matrix	Pixels	512 × 512
Resolution	Pixels/mm	0.59

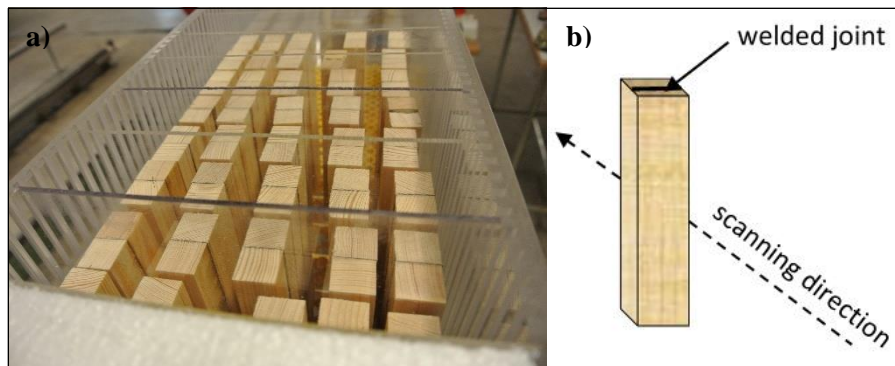


**Fig. 1.** a) Experimental rig for CT-scanning. Four batches of welded specimens were placed in the rigs and separated with plastic walls so that all the welded joints of each batch were placed along a line to be captured by a single scan; b) orientation of the specimens during scanning.

The CT scanning generates images with grayscale values that correspond to the attenuation coefficient of the materials. This coefficient is related to the density of the scanned material, as shown by an intensity profile (Lindgren *et al.* 1992; Vaziri *et al.* 2011). The MC of the scanned wood specimens can be determined by a complimentary scan of

the same specimens at 0% MC. The calculated X-ray linear attenuation coefficient ( $\mu_x$ ) in each small volume element (voxel) was normalized with respect to the corresponding linear attenuation coefficient for water ( $\mu_{\text{water}}$ ) (Herman 1980),

$$\text{CT-number} = 1000 \times \frac{\mu_x - \mu_{\text{water}}}{\mu_{\text{water}}} \quad (1)$$

where  $\mu_x$  is the attenuation coefficient for the tested material and  $\mu_{\text{water}}$  is the attenuation coefficient for water. A CT-number of -1000 indicates an object or a voxel within the object that has the density of air and a CT-number of zero indicates a region that has the density of water.

Water movement and crack propagation were traced in the direction perpendicular to the welding interphase by CT image analysis using the software Matlab® R2018b (The MathWorks, Inc., Natick, MA, USA). The positions of the welded joints were altered by the swelling of the specimens and were not along a line (Fig. 2). Therefore, the CT-number profiles of the specimens were created separately. After water absorption, the pick point of the CT-number profiles, which corresponded to the density of the weld joints, decreased below their original (dry) values, indicating a crack formed in the welded joints (Vaziri *et al.* 2011).

#### *X-ray micro-tomography scanning*

X-ray micro-tomography (also frequently referred to as micro CT) is a non-destructive radiographic imaging technique that can produce 3D images of a material's internal structure with a spatial resolution of less than 1  $\mu\text{m}$ . The largest specimen dimensions for which the highest resolution could be achieved without any serious defects in the weld interphase were 2 mm  $\times$  2 mm  $\times$  2 mm. Specimens of this size were prepared by slicing a thin section of the welded specimen and subdividing it with a microtome into needle-shaped pieces. The measurements were conducted at the micro-CT laboratory at the Luleå University of Technology (LTU) using a ZEISS Xradia 510 Versa system (Carl Zeiss AB, Stockholm, Sweden).

#### *Shear strength and water immersion*

To determine whether the wollastonite had any positive effects on the mechanical properties of the welded woods, four sets of specimens (each set consisting of nine replicates) were prepared to test the shear strength of the welded joint. The welded specimens were conditioned for ten days in an environmental chamber (20 °C and 65% RH) to 12% MC before testing. The specimens were cut in accordance with the European standard EN 14080 (2013). The specimens were tested using a universal testing machine (Instron; High Wycombe, Buckinghamshire, UK) in the longitudinal direction at a shear rate of 2 mm/min. The average and standard deviation of the bond strength and the average wood failure were calculated for each set of specimens (Table 3).

For the water immersion tests, the welded specimens with an original size of 20 mm  $\times$  20 mm  $\times$  200 mm were conditioned to 12% MC, and the conditioned specimens were then placed in tap water at ambient room temperature (22 °C) until delamination of the welded joints occurred.

## RESULTS AND DISCUSSION

### Crack Detection by CT scanning

Figure 2 shows the CT-number profile of two groups of specimens, that of the welded with and without wollastonite for 5 s, when a crack appeared in the welded joint of at least one of the specimens in comparison with their dry profiles (dotted lines in Fig. 2) and the previous time of scanning (dash-dotted lines in Fig. 2). Due to the swelling and the shrinkage of the wood, some variations occurred at the position of the welded joints. Specimens that were welded with wollastonite had a greater displacement (*i.e.*, swelling/shrinkage) than their corresponding controls.

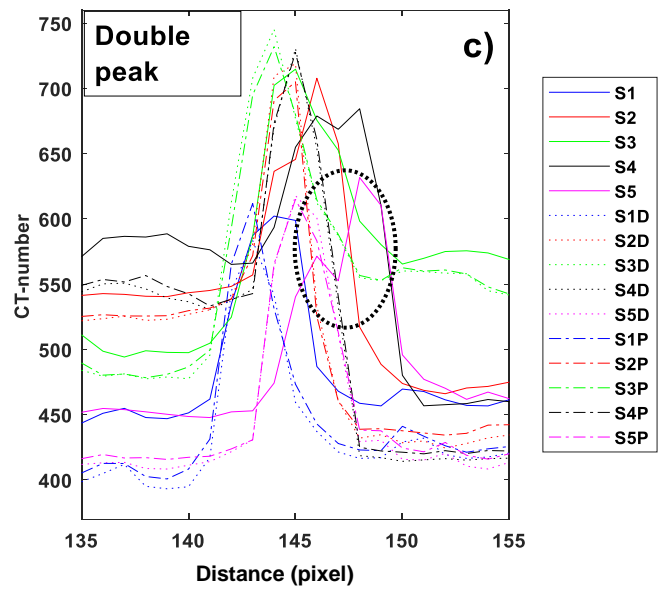
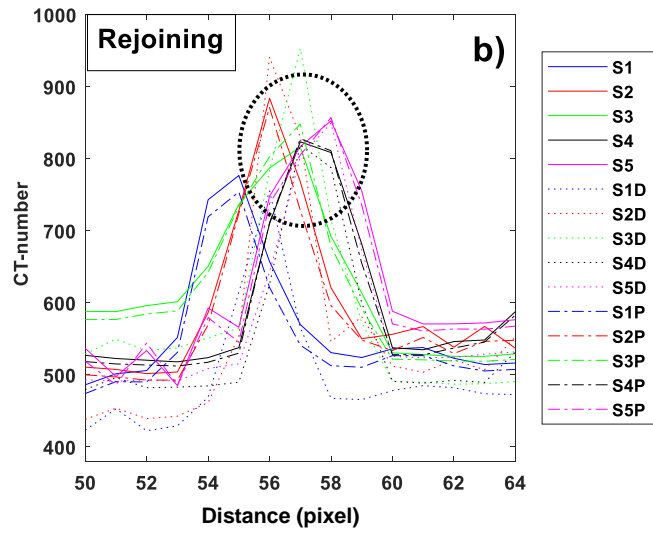
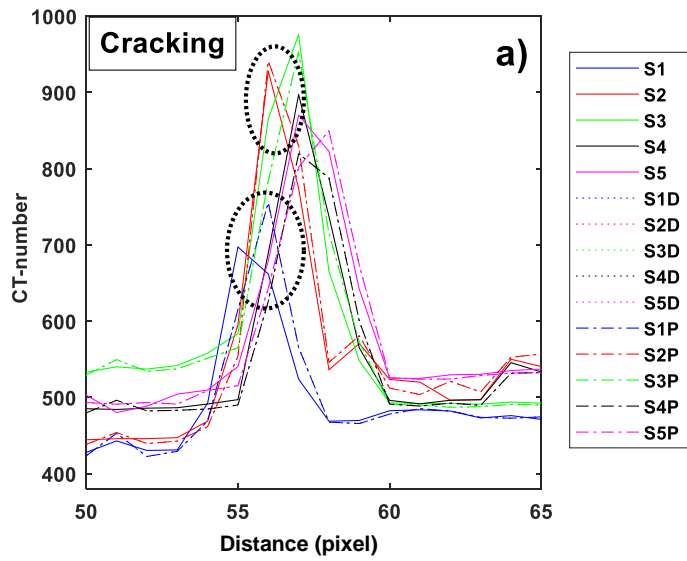
For the specimens welded with wollastonite, cracks developed with a zigzag pattern (double peak) on the top of the CT-number profiles (Fig. 2c), whereas for specimens welded without wollastonite a reduction in the top of the CT-number profiles indicated formation of a crack in the welded joint (Fig. 2a). The CT-numbers of some of the specimens (S1 and S2) welded without wollastonite (R5) decreased below their original (dry) values after 30 min in water, which indicated that a crack formed in the welded joints (dot ellipses in Fig. 2a). In contrast, one of the specimens (S5) welded with wollastonite (W5) did not crack until it was exposed to water for 2.5 h (dot ellipse in Fig. 2c).

The control specimens (R5) and specimens welded with wollastonite for 4 s (W4) had the shortest and longest average cracking times, respectively (Table 3). If the specimens R4, S1 and W4, S2 with the longest cracking times are considered experimental outliers, then the W5 group had the longest cracking time. The two way T-test indicated there was no statistically significant difference between the average cracking times within 95% confidence interval, but there was a tendency for the water resistance to increase (increasing the welding time) *via* welding with wollastonite.

**Table 3.** Average Cracking Time (h) for Five Replicates of Each Set of Specimens, Welded With and Without Wollastonite, as Detected by CT Image Analysis

Specimen Group No.	S1	S2	S3	S4	S5	Average	Average Without Experimental Outlier	Median
R4	31.5	2.5	0.5	2.5	2.5	7.9	2	2.5
R5	0.5	0.5	2.5	2.5	2.5	1.7		2.5
W4	0.5	96	0.5	0.5	10.5	21.6	3	0.5
W5	6.5	2.5	2.5	2.5	2.5	3.3		2.5

Despite the high density of wollastonite alone (average CT-number of 1400), the average CT-numbers of the welded joints with wollastonite were lower than those welded without wollastonite. This reduction may be explained by the small crystals of wollastonite that intruded between the wood pieces and created interstitial air pockets, which reduced the average density of the welded joint. The CT-number profiles of the joints of the specimens increased after cracking by continuing the water sorption and reached the same level as before or above (dotted ellipse in Figs. 2b and 2d). Sometimes secondary cracks were also observed. This may be explained by the cracks being filled with water or by swelling of the welded joint and/or wood around it and the re-joining of the wood pieces.



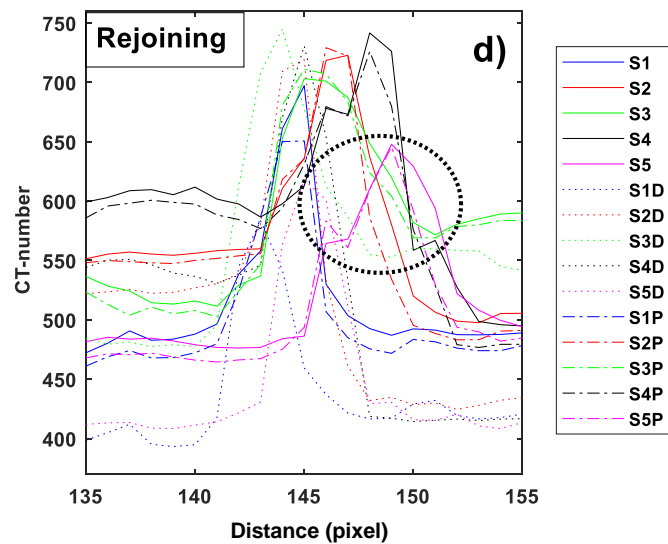


**Fig. 2.** CT-number profile of welded joints for two groups of specimens each consisting of five specimens: a) specimen welded without wollastonite (R5) after 30 min water sorption; b) specimen R5 after 6.5 h water sorption; c) specimen welded with wollastonite for 5 s (W5) after 2.5 h water sorption; and d) specimen W5 after 6.5 h water sorption. S1 to S5 denote the CT-number profile of the specimens at the scanning time; S1P to S5P denote the previous CT-number profiles (before the S1 to S5); and S1D to S5D denote CT-number profiles of the dry specimens (originals)

Wollastonite can improve the water resistance of the welded wood based on the CT-scanning results that contained the experimental outliers (Table 3). Specimens welded for a shorter time (W4) had a better performance than those welded for a longer time. In contrast, when considering the median values, the R4 performed appreciably lower than the other specimen sets. Using a high-resolution CT scanner and introducing different methods of crack detection may lead to different results than those obtained in this study.

### Water Resistance and Mechanical Strength Results

The average shear strength of the specimens welded with wollastonite was higher than that of the controls (Table 4); although the average shear strengths of the welded joints were acceptable, the percentage of wood failures were relatively low. Specimens welded for a longer time (W5) exhibited the maximum average shear strength. The alkaline wollastonite contains no acidic compounds, which can create an acidic environment that leads to a loss of mechanical wood strength (White 1979). The wollastonite particles may participate as reinforcing agents in the nanocomposite structure at the welded interphase area and lead to an enhanced shear strength.

**Table 4.** Average Shear Strength of the Specimens

Specimen Type	Average Shear Strength (MPa)	Maximum Shear Strength (MPa)	Wood Failure (%)
W5	7.41 ± 3.32	12	20
R5	6.3 ± 3.31	11.8	10
W4	6.4 ± 2.05	10	10
R4	4.93 ± 2.3	9.8	5



carbohydrate, which involved the production of furfurals and levoglucosan, as well as phenols during lignin degradation.

Condensation reactions between the aldehydes and the phenols may take place during the welding process, which results in the formation of cured resins when exposed to heat and alkaline or acid conditions. Formation of a more condensed matrix of these composite materials around the wollastonite particles may enhance the resistance of the welded joint to water. Once the most important questions have been answered, future work should expose the welded specimens to extreme weather variation, such as those found in Northern Europe, for a couple of months with testing at regular intervals. It is also recommended that future work should study the cracking times and water resistances of more specimens welded for different times to obtain a clear correlation among these parameters. This study provided new knowledge to enhance the moisture resistance of welded wood joints.

### Micro CT Scanning

The micro CT images of four typical specimens are shown in Fig. 4. The effect of end-grain direction on the welded joint structure is also shown. The growth rings contained alternate layers of earlywood, which has a low density, and latewood, which has a high density that is several times greater. Figure 4a shows in the radial surface of the welded interphase more or less perpendicular to the growth rings, the earlywood with larger tracheid cells were exposed to intense degradation by welding, whereas latewood with narrower and smaller tracheid cells remained almost intact.

The uneven degradation of the tracheids resulted in a welded joint with varying thickness. The welds were thicker around the earlywood and thinner around the latewood, which gave a wavy appearance to the overall joint in the cross-section of the welded specimen (Fig. 5). This structure of the growth rings consists of alternate weak and strong layers across the growth ring that lead to an accumulation of wollastonite particles around earlywood and an uneven dispersion of the particles through the welded interphase (Fig. 4d). Increasing the welding time resulted in an increase in the interfacial temperature (Vaziri *et al.* 2014), which led to the softening of the middle lamella and to the increased thickness of the welded joint. The flow-induced material at the interphase led to a fairly homogeneous distribution of the wollastonite particles throughout the weld interphase (Fig. 4f).

The end-grain direction of the specimens was tangential-radial. The pieces of wood that are cut along the tangential plane swell, contract, and become distorted at twice the rate of those cut along the radial plane (Stamm 1964). It seemed that the latter also withstood more tearing and rubbing caused by the welding, especially when the tree has been growing slowly resulting in tightly concentrated growth rings with a larger proportion of the harder latewood. This applied to pure tangential or radial ring orientation, which rarely occurred in commercial lumber where the growth rings are seldom aligned parallel or perpendicular to the board faces.

Welding the wood pieces along the end-grain-to-end-grain direction of the radial face-to-radial face (0° butt joint) should result in homogeneously welded joints that readily swells and dries with little degradation, and that has good dimensional stability.

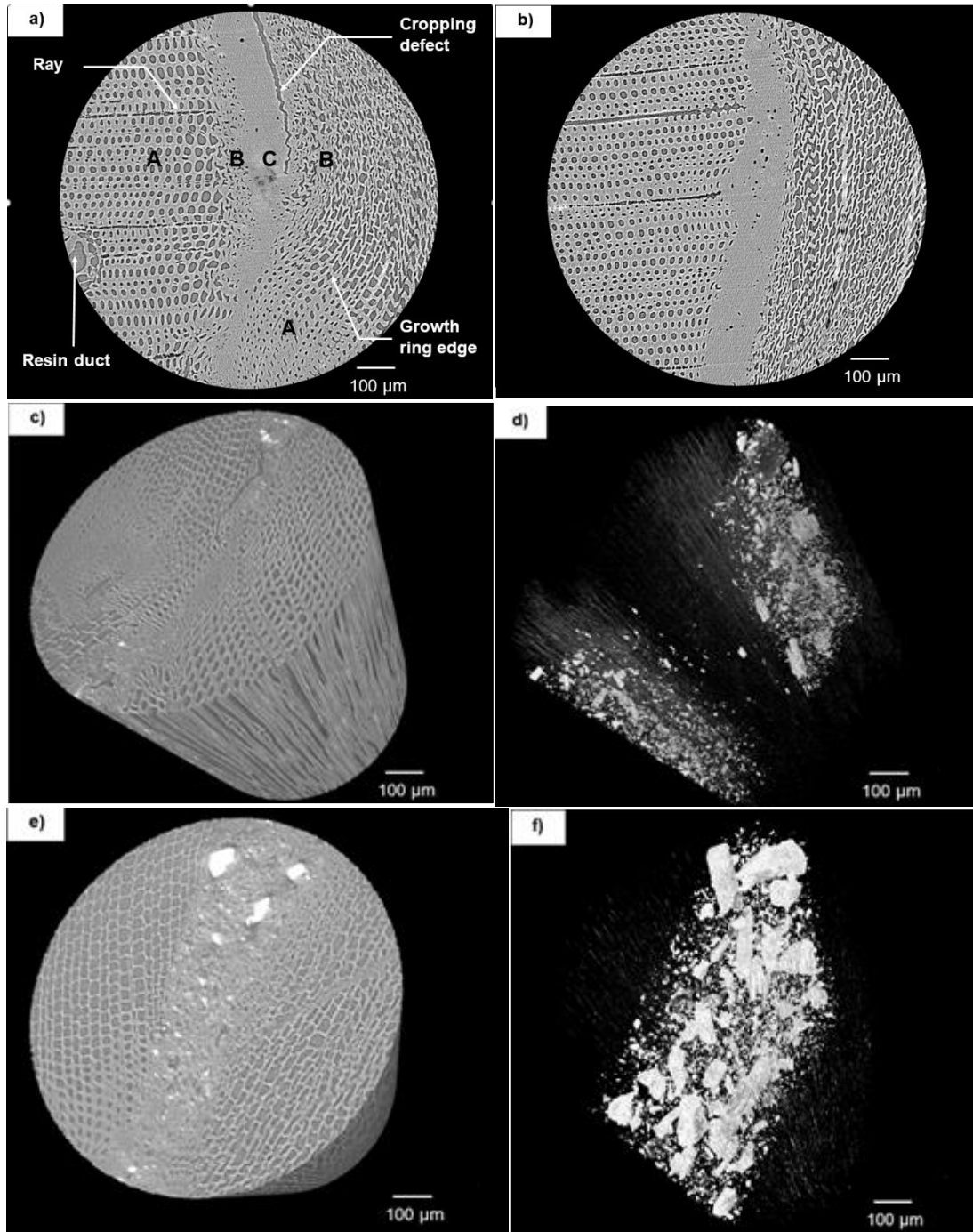


**Fig. 4.** X-ray computed micro-tomography images of transverse sections of pine specimens: a) welded without wollastonite for 4 s (R4); b) welded without wollastonite for 5 s (R5); c) 3D view of the specimens welded with wollastonite for 4 s (W4); d) distribution of the wollastonite particles within the welded joint of W4; e) 3D view of the specimens welded with wollastonite for 5 s (W5); and f) distribution of the wollastonite particles within the welded joint of W5 with a slight rotation of the specimen. The three zones marked in Fig. 4a denote latewood (A), compressed tracheid of earlywood close to the welded interphase (B), and welded joint (C). The radial surface of the welded interphase is located to the right and the tangential surface is located to the left; all specimens had some slope of the grain. Figure 4a also shows a micro-crack that was created when preparing the specimens.

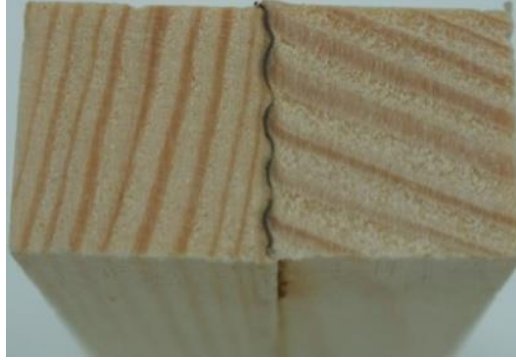


**Fig. 5.** Zigzag or finger-joint pattern of the welded joint on the cross-section of a welded specimen

## CONCLUSIONS

1. Welding with wollastonite increased the time to cracking of the welded Scots pine joints. Increasing the welding time tended to increase the water resistance and to improve the shear strength of the welded wood. This effect was further improved by welding with wollastonite.
2. Wollastonite particles can contribute to the formation of an effective welded joint by participating as reinforcing agents in the nanocomposite structure at the welded interphase areas. Wollastonite can also increase the friction at the weld's interphase, which in turn can make a matrix of insoluble dehydration products around wollastonite particles and increase resistance of the welded joint to water.
3. The incompatibility among the results from CT-scanning, water immersion, and shear strength tests suggested that the cracking time might not be an indicator of the durability and strength of the welded wood. Because specimens containing cracks were still able to withstand the water immersion without delamination, it was concluded that the size, depth, and distribution of the cracks also had some effect on the water resistance of the welded wood.
4. The microstructure of the welded specimens showed that the added wollastonite became more evenly distributed in the welded joint in the specimens welded for a relatively long time (5 s).
5. The results of this study indicated that a joint might be able to withstand climatic variations when placed outdoors.

## ACKNOWLEDGMENTS

Financial support from the Swedish Research Council for Environment, Agricultural Sciences and Spatial Planning (FORMAS), project Wood Welding - "Glue-free Wood Assembly 2017-01157", is gratefully acknowledged. The authors also express their thanks to Rob Hellingwelf, Professor of Ore Geology, Certified EU Geologist, and Adjunct Professor at the Luleå University of Technology, for providing the wollastonite.

## REFERENCES CITED

- Amirou, S., Pizzi, A., and Delmotte, L. (2017). "Citric acid as waterproofing additive in butt joints linear wood welding," *Holz als Roh-und Werkstoff* 75(4), 651-654. DOI: 10.1007/s00107-017-1167-x
- EN 14080 (2013). "Timber structures – Glued laminated timber and glued solid timber requirements," European Committee for Standardization, Brussels, Belgium.
- Herman, G. T. (1980). *Image Reconstruction from Projections: The Fundamentals of Computerized Tomography*, Academic Press, New York, NY, USA.
- Karimi, A., Taghiyari, H. R., Fattahi, A., Karimi, S., Ebrahimi, G., and Tarmian, A. (2013). "Effects of wollastonite nanofibers on biological durability of poplar wood (*Populus nigra*) against *Trametes versicolor*," *BioResources* 8(3), 4134-4141. DOI: 10.15376/biores.8.3.4134-4141
- Lindgren, O., Davis, J., Wells, P., and Shadbolt, P. (1992). "Non-destructive wood density distribution measurements using computed tomography," *Roh-und Werkstoff* 50(7-8), 295–299. DOI: 10.1007/BF02615356
- Mansouri, H. R., Pizzi, A., Leban, J. M., Delmotte, L., Lindgren, O., and Vaziri, M. (2011). "Causes for the improved water resistance in pine wood linear welded joints," *Journal of Adhesion Science and Technology* 25(16), 1987-1995. DOI: 10.1163/016942410X544794
- Maxim, L. D., and McConnell, E. E. (2005). "A review of the toxicology and epidemiology of Wollastonite," *Inhalation Toxicology* 17(9), 451-466. DOI: 10.1080/08958370591002030
- Pizzi, A., Mansouri, H. R., Leban, J. M., Delmotte, L., and Pichelin, F. (2011). "Enhancing the exterior performance of wood joined by linear and rotational welding," *Journal of Adhesion Science and Technology* 25(19), 2717-2730. DOI: 10.1163/016942411X556088
- Shepp, L. A., and Logan, B. F. (1974). "The Fourier reconstruction of a head section," *IEEE Transactions on Nuclear Science* 21(3), 21-43. DOI: 10.1109/TNS.1974.6499235
- Stamm, A. J. (1964). *Wood and Cellulose Science*, Ronald Press Co., New York, USA.
- Vaziri, M., Berg, S., Sandberg, D., and Gheinani, I. T. (2014). "Three-dimensional finite element modelling of heat transfer for linear friction welding of Scots pine," *Wood Material Science and Engineering* 9(2), 102-109. DOI: 10.1080/17480272.2014.903297
- Vaziri, M., Lindgren, O., and Pizzi, A. (2011). "Influence of welding parameters and wood properties on the water absorption in Scots pine joints induced by linear welding," *Journal of Adhesion Science and Technology* 25(15), 1839-1847. DOI: 10.1163/016942410X525731
- Vaziri, M., Karlsson, O., and Sandberg, D. (2019a). "Wetting characteristic of welded wood. Part 1. Determination of apparent contact angle, swelling, and liquid sorption," *Holzforschung* (submitted).
- Vaziri, M., Karlsson, O., and Sandberg, D. (2019b). "Wetting characteristic of welded wood. Part 2. Effect of wollastonite," *Holzforschung* (submitted).

Article submitted: October 2, 2019; Peer review completed: December 8, 2019; Revised version received and accepted: January 15, 2020; Published: January 17, 2020.  
DOI: 10.15376/biores.15.1.1617-1628